

Surface defects in the $O(N)$ model

Maxime Trépanier*

*Department of Mathematics, King's College London,
London, WC2R 2LS, United Kingdom*

Abstract

I study the two-dimensional defects of the d dimensional critical $O(N)$ model and the defect RG flows between them. By combining the ϵ -expansion around $d = 4$ and $d = 6$ as well as large N techniques, I find new conformal defects and examine their behavior across dimensions and at various N . I discuss how some of these fixed points relate to the known ordinary, special and extraordinary transitions in the 3d theory, as well as examine the presence of new symmetry breaking fixed points preserving an $O(p) \times O(N - p)$ subgroup of $O(N)$ for $N \leq N_c$ (with the estimate $N_c = 6$). I characterise these fixed points by obtaining their conformal anomaly coefficients, their 1-point functions and comment on the calculation of their string potential. These results establish surface operators as a viable approach to the characterisation of interface critical phenomena in the 3d critical $O(N)$ model.

arXiv:2305.10486v3 [hep-th] 11 Sep 2023

*trepanier.maxime@gmail.com

1 Introduction and summary

The problem of classifying boundaries and interfaces of the 3d critical $O(N)$ model has attracted considerable attention since the pioneering works of [1–4]. The critical exponents characterising some of the possible boundary phases were obtained early on through a combination of field theory techniques and found experimental verification in phenomena such as the critical adsorption of fluids on walls [5–9], see [10] for an early review. Yet, still today the characterisation of the various phases and their organisation into a phase diagram for general N is not settled [11, 12].

Although the $d = 3$ critical $O(N)$ model is the most interesting for describing physical systems, it is not directly accessible to perturbative methods and the theory is often studied by analytically continuing d to the range $2 < d < 6$. In this context it is an interesting question to understand how to describe boundaries and interfaces away from $d = 3$. The most established method to do so is to study boundaries/interfaces in d dimensions, which corresponds to keeping the codimension of the defect fixed. For boundaries this is dictated by the topology of spacetime and that approach has been the subject of numerous works such as [2, 4, 13–16]. For interfaces, however, there is another natural choice: we can keep the dimension of the defect fixed and study surface defects in the d dimensional $O(N)$ model.¹ This is the focus of this paper.

The origin of these surface defects is easy to explain. In any CFT, we may consider a set of local operators \mathcal{O}_I with conformal dimension $\Delta_{\mathcal{O}_I}$ and construct a defect by integrating local operators over a plane with some coupling constants u^I to be fixed shortly

$$D = \exp \left[- \int_{\mathbb{R}^2} d^2\tau u^I \mathcal{O}_I \right]. \quad (1.1)$$

Unless the operators have $\Delta_{\mathcal{O}_I} = 2$ exactly, the couplings u^I get renormalised and give rise to a defect RG flow (dRG flow). The beta function that governs their renormalisation near the trivial defect $u^I = 0$ is well understood and given by [17, 18]

$$\beta_{u^I} = (\Delta_{\mathcal{O}_I} - 2)u^I + \pi C^I_{JK} u^J u^K + \dots \quad (1.2)$$

where C_{IJK} are the structure constants of the bulk theory for \mathcal{O}_I and the indices are raised by the Zamolodchikov metric for \mathcal{O}_I . The nontrivial zeros u^I_* of this beta function then correspond to nontrivial conformal surface defects.

In this paper, I undertake the exploration of surface defects and their dRG flows in the $O(N)$ model through perturbative methods. By combining the ϵ -expansion as well as exploiting large N techniques, I uncover a rich structure of dRG flows and fixed points corresponding to new defects, as well as phenomena such as the appearance/annihilation of fixed points as we vary the parameters d and N .

The simplest setting in which one can study surface defects is perhaps at $d = 4 - \epsilon$ using the ϵ -expansion, and this is presented in section 2. There, surface defects naturally arise from integrating the operator $\varphi^i \varphi^j$ over a plane as in (1.1) ($i = 1, \dots, N$). In addition to the $O(N)$ symmetric defect D_N coupling to $\varphi^k \varphi^k$, I find fixed points corresponding to conformal defects D_p preserving a subgroup $O(p) \times O(N - p)$ of the full $O(N)$ symmetry (with $0 \leq p \leq N$). These defects have an analog in the free $O(N)$ model analysed in [19],

¹This applies to “topologically trivial” interfaces, where we have a copy of the $O(N)$ model of each side of the defect.

where one can engineer a conformal defect preserving the same symmetry by taking p scalars at one zero of the beta function ($u_* = \pi\epsilon$) and the rest at the other ($u_* = 0$). As for the free theory, these defects can be thought of as saddle points of a symmetry breaking dRG flow, with the stable fixed point the symmetry preserving defect D_N . Surprisingly however, here the symmetry breaking fixed points only exist for small enough $N \leq N_c$, with $N_c = 6$, to first order in ϵ .

Away from $d = 4$ these defects can be reliably studied using the large N expansion. In section 3 I examine the behavior of the stable fixed point D_N across dimensions. This is particularly simple when studying the theory through the Hubbard-Stratonovich transformation, as the defect couples directly to the Hubbard-Stratonovich field σ . Taking $d \rightarrow 3$ leads to a divergence in the defect coupling u_* (the zero of the beta function of the coupling to σ), which signals a change of scaling with respect to N . I argue that D_N becomes the fixed point of the well-known ordinary transition in $d = 3$, while the trivial defect is known to be the special transition [1].

In addition to the ordinary and special transitions, the 3d $O(N)$ model has the extraordinary (or normal) transition, which is characterised by its breaking of $O(N)$ symmetry to $O(N - 1)$. A setup with perturbative control to study this defect is the ϵ -expansion around $d = 6$, where the breaking is naturally realised by coupling the defect to a fundamental scalar φ^1 . This is the analog of the pinning defect studied in the context of line operators [20]. We find that near $d = 6$ the fixed point corresponds to a non-unitary surface defect, at least at large N . It is interesting to note that the same is true of the boundary defect describing the extraordinary fixed point around $d = 6$ [21].

It is rather encouraging to recover the known classes of interfaces at $d = 3$ directly from surface defects: it suggests that surface defects are a viable alternative to describing interface critical phenomena in $d = 3$. Now, studying surface operators instead of boundaries has certain advantages. The main property of surface defects (and indeed interfaces in $d = 3$) is their conformal anomaly governing the UV divergences of their expectation value, here this is manifest for any d . For a surface defect D_Σ defined over a surface Σ inside a d -dimensional manifold of metric G , the expectation value receives a universal contribution of the form [22]

$$\log \langle D_\Sigma \rangle = \frac{\log \tilde{\epsilon}}{4\pi} \int \text{vol}_\Sigma \left[a\mathcal{R}^\Sigma + b_1 \text{tr} \tilde{\mathbb{I}}^2 + b_2 \text{tr} W + c(\partial n)^2 \right] + \text{finite}, \quad (1.3)$$

where $\tilde{\epsilon}$ is a UV cutoff, \mathcal{R}^Σ is the 2d Ricci scalar on Σ , $\tilde{\mathbb{I}}$ is the traceless part of the second fundamental form squared, $\text{tr} W$ is the trace of the pullback of the Weyl tensor on Σ , and $(\partial n)^2$ is a term relevant for symmetry breaking surfaces; its precise form is given in section 5. Note that in $d = 3$ the Weyl tensor vanishes identically and that term is absent. A review of the geometric invariants and the various basis used for conformal anomalies can be found in [23] (see also [24]).

The anomaly coefficients a, b_1, b_2, c do not depend on the geometry, but may depend on d, N . They are particularly interesting because they are constrained by unitarity and appear in a wide variety of observables. Perhaps most importantly, the coefficient a is known to obey an a -theorem [25] (see also [26, 19])

$$a_{UV} > a_{IR}, \quad (1.4)$$

which provides an important diagnosis of dRG flows. The perturbative dRG flows presented below provide new nontrivial examples where the a -theorem applies and is indeed satisfied.

More interesting are the cases where the perturbative analysis falls short—still we expect that the IR fixed point corresponds to the defect with lowest value of a allowed by symmetry.

The coefficients b_1, b_2, c are also constrained by unitarity to have definite signs. b_1 and c are respectively associated to the displacement operator \mathbb{D} (tilt operator \mathbb{O}) arising from the breaking of translation symmetry (resp. the $O(N)$ symmetry). Concretely, the displacement operator appears as a contact term for the conservation law of the stress tensor along a direction orthogonal to the defect x_\perp^m (I write $D[\hat{\mathcal{O}}]$ to denote the insertion of the local operator $\hat{\mathcal{O}}$ on the defect D)

$$\partial_\mu T^{\mu m}(x)D = D[\mathbb{D}^m(x_\parallel)]\delta^{(d-2)}(x_\perp). \quad (1.5)$$

A similar equation defines the tilt operator from the $O(N)$ symmetry current j^μ . Since (1.5) fixes the normalisation of \mathbb{D} , the coefficient $C_{\mathbb{D}}$ appearing in the 2-point function $\langle D[\mathbb{D}^m(\sigma)\mathbb{D}^n(0)] \rangle$ is an observable, and is known to satisfy $-b_1 \sim C_{\mathbb{D}} > 0$ [27]. Similarly $c \sim C_{\mathbb{O}} > 0$ [28].

Finally b_2 is related to the 1-point function of stress tensor [29] (see also [30, 27]), and by the ANEC is expected to satisfy $b_2 > 0$ [29].

I calculate the anomaly coefficients for the various defects studied here in section 5. There are other quantities associated to surface defects, and two more observables play a role in this paper. The first one is the 1-point function of φ^2 in the presence of the defect. The quantity that is independent of the normalisation of φ^2 (thus can be compared between various calculations) is a_{φ^2}

$$\frac{\langle \varphi^2(x)D|_{u_*} \rangle}{\sqrt{C_{\varphi^2}} \langle D|_{u_*} \rangle} = \frac{a_{\varphi^2}}{|x_\perp|^{\Delta_{\varphi^2}}}, \quad \langle \varphi^2(x)\varphi^2(0) \rangle = \frac{C_{\varphi^2}}{|x|^{2\Delta_{\varphi^2}}}. \quad (1.6)$$

Giving a VEV to φ^2 is akin to sourcing a mass term for φ (here localised at the defect), with a positive mass corresponding to $a_{\varphi^2} \leq 0$. The agreement of a_{φ^2} between various calculations is a nontrivial cross-check of these results.

The second quantity of interest is the generalised string potential introduced in [31], which is analogous to the cusp anomalous dimension of line operators. In particular this captures the potential density U_0 between a pair of planar defects separated a distance L , i.e. $\langle D|_{u_*}(L)D|_{u_*}(0) \rangle = \frac{U_0 \text{Area}}{L^2}$.

The rest of this paper is organised as follows. Sections 2, 3 and 4 present three limits where perturbative methods can be applied to study surface defects, and are devoted to studying dRG flows and characterising fixed points. Section 5 contains the calculation of the anomaly coefficients and the string potential. In order to alleviate the reading of the paper, the perturbative calculations are relegated to appendix A.

Note added: Shortly after this paper appeared on the arXiv, I learned of related works to appear [32] and [33], which overlap with parts of this paper. I am grateful to the authors for informing me of their work and sharing a preview of their papers with me.

2 ϵ -expansion in $d = 4 - \epsilon$

Consider the critical $O(N)$ model. In $d = 4 - \epsilon$ this model can be studied in renormalised perturbation theory from the action

$$S = \int d^{4-\epsilon}x \left[\frac{1}{2} (\partial_\mu \varphi^i)^2 + \frac{M^\epsilon \lambda}{4!} (\varphi^i \varphi^i)^2 \right], \quad (2.1)$$

where M is the renormalisation scale and we omitted the counterterms. The theory becomes conformal when tuning the coupling constant to its critical point

$$\frac{\lambda_*}{(4\pi)^2} = \frac{3}{N+8} \epsilon + O(\epsilon^2). \quad (2.2)$$

We can construct a surface operator in this theory by integrating $\varphi^i \varphi^j$ over a surface²

$$D = \exp \left[-\frac{M^\epsilon}{2} \int_{\mathbb{R}^2} d^2\tau h_{ij} \varphi^i \varphi^j \right], \quad (2.3)$$

where we included an explicit dependence on the renormalisation scale M to ensure that h_{ij} is dimensionless.

The coupling h_{ij} gets renormalised and obeys the beta function (1.2). This is easy to see in perturbation theory. To lowest order, there are three diagrams contributing to the renormalisation of the coupling. They can be evaluated in dimensional regularisation using standard methods (see appendix A for details) and read

$$\begin{array}{c} \text{---} \\ \bullet \\ \text{---} \\ \vdots \end{array} = -\frac{h_{ij}}{16\pi^3 x_\perp^2} + \dots, \quad (2.4)$$

$$\begin{array}{c} \text{---} \\ \bullet \\ \text{---} \\ \text{---} \\ \bullet \\ \text{---} \end{array} = \frac{\lambda}{(4\pi)^2} \frac{(h_{kk} \delta_{ij} + 2h_{ij})}{24\pi^3 x_\perp^2} \left[\frac{1}{\epsilon} + \frac{4 + 3\gamma + 3 \log(\pi M^2 x_\perp^2)}{2} + \dots \right], \quad (2.5)$$

$$\begin{array}{c} \text{---} \\ \bullet \\ \text{---} \\ \text{---} \\ \bullet \\ \text{---} \end{array} = \frac{h_{ik} h_{kj}}{32\pi^4 x_\perp^2} \left[\frac{1}{\epsilon} + \frac{4 + 3\gamma + 3 \log(\pi M^2 x_\perp^2)}{2} + \dots \right]. \quad (2.6)$$

Here the dashed lines are propagators for φ^i , while the solid line represents an integral over the plane supporting the defect. γ is the Euler constant.

The poles in ϵ are absorbed by counterterms and ensure that the expectation value of the composite operator $[\varphi^i \varphi^j]$ is finite, see the corresponding diagrams in table 2. The divergence of the second diagram is cancelled by the renormalisation of $[\varphi^i \varphi^j]$, which in terms of irreducible representations—singlet S and symmetric traceless T —are given by (see e.g. [34])

$$Z_S = 1 - \frac{\lambda}{(4\pi)^2} \frac{N+2}{3} \frac{1}{\epsilon} + \dots, \quad Z_T = 1 - \frac{\lambda}{(4\pi)^2} \frac{2}{3} \frac{1}{\epsilon} + \dots \quad (2.7)$$

The remaining pole of (2.6) can be cancelled by the counterterm δh_{ij}

$$\delta h_{ij} = \frac{1}{\epsilon} \frac{h_{ik} h_{kj}}{2\pi} + O(h^2 \lambda, h^3). \quad (2.8)$$

²More generally, one may also include the relevant operator $u^i \varphi^i$. We discuss such defects in $d = 6 - \epsilon$ in section 4 where the dRG flows are easily accessible to perturbative methods.

From these counterterms we can read the beta function for the coupling h_{ij} . Decomposing $h_{ij} = h^S \delta_{ij} + h_{ij}^T$ in irreducible representations, the renormalised couplings $h^{S,T}$ are related to the bare coupling $(h^{S,T})^{(0)}$ by

$$(h^S)^{(0)} = M^\epsilon (h^S + \delta h^S) Z_S^{-1/2}, \quad (h_{ij}^T)^{(0)} = M^\epsilon (h_{ij}^T + \delta h_{ij}^T) Z_T^{-1/2}. \quad (2.9)$$

Using that bare couplings $h^{(0)}$ are independent of the renormalisation scale M , one can easily obtain the beta functions for h^S and h^T (see e.g. the review [35], or [20] in the context of defects). Assembling both representations we get

$$\beta_{h_{ij}} = -\epsilon h_{ij} + \frac{\lambda}{(4\pi)^2} \frac{h_{kk} \delta_{ij} + 2h_{ij}}{3} + \frac{1}{2\pi} h_{ik} h_{kj} + O(h^3, h^2 \lambda, h \lambda^2). \quad (2.10)$$

This result can be compared with (1.2). The terms linear in h combine to give the conformal dimension as expected (for reference, the dimensions of $[\varphi^i \varphi^j]$ are $\Delta_S = 2 - \frac{6}{N+8} \epsilon + \dots$ and $\Delta_T = 2 - \frac{N+6}{N+8} \epsilon + \dots$ respectively for the singlet and symmetric traceless representations [34]). In both cases, $\Delta < 2$ so the operator is relevant and triggers an RG flow.

The term quadratic in h reproduces the structure constant of $[\varphi^i \varphi^j]$. For this calculation we only need the leading order contribution in ϵ and neglect λ corrections, so they are given by the structure constant of the free $O(N)$ model, see e.g. [19].

In the following we determine the fixed points of the beta function (2.10) corresponding to conformal surface defects.

2.1 Symmetry preserving defect

The simplest fixed points of the beta function correspond to defects preserving the full $O(N)$ symmetry, for which we should take $h_{ij} = h_N \delta_{ij}$. Substituting this ansatz into the beta function and plugging the value of $\lambda = \lambda_*$ (2.2) we get two zeros

$$\frac{h_{N,+}}{2\pi} = \frac{6\epsilon}{N+8} + O(\epsilon^2), \quad h_{N,-} = 0. \quad (2.11)$$

The case $h_{N,-}$ is the trivial defect D_0 , while $h_{N,+}$ is a new nontrivial surface defect I call D_N . The RG flow between these two fixed points is driven by the defect operator $\hat{\sigma} \sim \varphi_S^2$ (up to a normalisation factor), which is relevant in D_0 . At D_N its conformal dimension can be obtained from the derivative of the beta function [36] and is irrelevant

$$\hat{\Delta}_{\hat{\sigma}} = 2 + \beta'(h)|_{h_{N,+}} = 2 + \frac{6\epsilon}{N+8} + \dots \quad (2.12)$$

These defects are characterised by their sourcing of φ_S^2 , which is encoded in the dCFT coefficient a_{φ^2} appearing in (1.6). We read it from (2.4)

$$a_{\varphi^2} = -\frac{N h_{N,+}}{16\pi^3 \sqrt{C_{\varphi_S^2}}} = -\frac{3\sqrt{N}\epsilon}{\sqrt{2}(N+8)} + O(\epsilon^2), \quad C_{\varphi_S^2} = \frac{N}{8\pi^4} + O(\epsilon). \quad (2.13)$$

2.2 Breaking to $O(p) \times O(N - p)$

A natural generalisation is to allow surface operators to break the $O(N)$ symmetry, and we start by discussing the breaking to the subgroup $O(p) \times O(N - p)$. It turns out that, at this order in the ϵ -expansion there are no fixed points breaking more symmetries, so this is already the most general case (we return to this question in section 2.3).

To simplify our analysis, we use the $O(N)$ symmetry to diagonalise h_{ij} to its set of eigenvalues, and take p eigenvalues of value h_p and $N - p$ eigenvalues of value h_{N-p} . Decomposing the beta function (2.10) for the diagonal elements h_p and h_{N-p} of h_{ij} , the vanishing of the beta functions reduces to³

$$\beta_{h_p} = -\epsilon h_p + \frac{\lambda}{(4\pi)^2} \frac{(p+2)h_p + (N-p)h_{N-p}}{3} + \frac{h_p^2}{2\pi} + \dots = 0, \quad (2.14)$$

$$\beta_{h_{N-p}} = -\epsilon h_{N-p} + \frac{\lambda}{(4\pi)^2} \frac{ph_p + (N+2-p)h_{N-p}}{3} + \frac{h_{N-p}^2}{2\pi} + \dots = 0, \quad (2.15)$$

with the ellipsis containing terms subleading in ϵ .

The fixed points. The solutions to these equations are easily obtained. The beta functions are exchanged under the relabelling $p \rightarrow N - p$, so $\beta_{h_p} - \beta_{h_{N-p}}$ is odd with respect to that symmetry and is given by

$$\beta_{h_p} - \beta_{h_{N-p}} = (h_p - h_{N-p}) \left(\frac{h_p + h_{N-p}}{2\pi} - \epsilon + \frac{2\lambda}{3(4\pi)^2} + \dots \right) = 0. \quad (2.16)$$

In the symmetry breaking case, we require $h_p \neq h_{N-p}$. This fixes $h_p + h_{N-p}$, and substituting into $\beta_{h_p} + \beta_{h_{N-p}}$ we can solve for $h_p - h_{N-p}$. The solution is given by the pair $\{h_{p,+}, h_{N-p,-}\}$, where

$$\frac{h_{p,\pm}}{2\pi} = \frac{(N+3-p) \pm \Delta}{N+8} \epsilon, \quad \Delta^2 = 9 - p(N-p). \quad (2.17)$$

The choice of sign for the square root gives rise to 2 different solutions for any given p , and for simplicity here we used the freedom to relabel $p \rightarrow N - p$ to choose a definite sign. As a consistency check, we recover the symmetry preserving defect D_N defined in (2.11) by setting $p = N$, and the trivial defect D_0 by setting $p = 0$.

The properties of these fixed points are controlled by the sign of the discriminant Δ^2 . For N below the critical value $N_c = 6$, the discriminant is positive and the h 's are real numbers: these are fixed points of the dRG flow preserving an $O(p) \times O(N - p)$ symmetry, and they correspond to conformal defects which I call D_p .

Above the critical bound $N > N_c$, there are values of p for which the discriminant is negative. This happens for $1 < p < N - 1$ for $6 < N \leq 10$, and $0 < p < N$ for $N > 10$ (for integer p). In that case, (2.17) describes complex fixed points of the beta function. In a unitary theory, the h 's remain real along dRG flows, so these fixed points are not reached by a dRG flow (they may however lead to walking behavior as in [37]).

At certain values of $p(N)$ the discriminant vanishes exactly, so that $h_{p,+} = h_{p,-}$ and the defects D_p and D_{N-p} become degenerate. This happens at integer values of p for $N = 6$

³One can also decompose the beta function in terms of irreducible representations of $O(N)$, but it does not lead to a factorisation of the equations because of the explicit symmetry breaking.

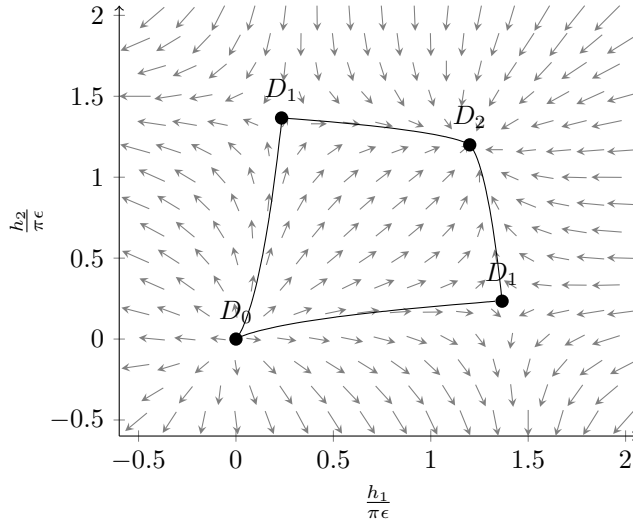


Figure 1: Example of a defect RG flow for surface defects in the $O(2)$ model. The vector field is $-\beta(h_1, h_2)$ given in terms of the eigenvalues h_1, h_2 . There is a \mathbb{Z}_2 symmetry exchanging $h_1 \leftrightarrow h_2$. The 3 fixed points are D_0, D_1 and D_2 , their values of h 's are given in (2.17). The black lines indicate the stable manifold.

($p = 3$) and $N = 10$ ($p = 1, 9$). In fact, for $N = 6$ one can check that the fixed points (2.17) have the same values of h for $p = 3, 4, 5, 6$, so that all four defects D_p become degenerate and coincide with the symmetry preserving defect (2.11). As far as I know this is the first example of a simultaneous collision of four fixed points! It would be interesting to see if this degeneracy is lifted at subleading orders in ϵ .

We can gather more information about the structure of the dRG flow from the beta function (2.10). The eigenvalues of its jacobian give the conformal dimension of defect operators involved in the flow. There are four different eigenvalues, which correspond to four defect operators:

Operator	$O(p)$	$O(N-p)$	$\hat{\Delta} - 2$
$\hat{\mathcal{O}}_{S,+}$	S	S	$\frac{\epsilon}{2(N+8)} \left[N + \sqrt{N^2 + 8(N-2p)\Delta + 16\Delta^2} \right]$
$\hat{\mathcal{O}}_{S,-}$	S	S	$\frac{\epsilon}{2(N+8)} \left[N - \sqrt{N^2 + 8(N-2p)\Delta + 16\Delta^2} \right]$
$\hat{\mathcal{O}}_{T,+}$	T	S	$\frac{N-2p+2\Delta}{N+8} \epsilon$
$\hat{\mathcal{O}}_{T,-}$	S	T	$-\frac{N-2p+2\Delta}{N+8} \epsilon$

Table 1: List of defect operators involved in the dRG flow for the defect D_p , their representation (singlet S /traceless symmetric T) and their conformal dimension $\hat{\Delta}$. Note that $\hat{\mathcal{O}}_{S,+}$ is absent when $p = 0$, $\hat{\mathcal{O}}_{S,-}$ when $p = N$, $\hat{\mathcal{O}}_{T,+}$ when $p < 2$ and $\hat{\mathcal{O}}_{T,-}$ is absent when $N - p < 2$.

The operators relevant for assessing the stability of the fixed points are $\hat{\mathcal{O}}_{S,\pm}$. Notice that for $N \leq 6$, $\hat{\mathcal{O}}_{S,-}$ is a relevant defect operator (i.e. $\hat{\Delta} < 2$) present in all defects D_p except the symmetry preserving defect D_N . Therefore we expect a dRG flow between the defects $D_0 \rightarrow D_p \rightarrow D_{N-p} \rightarrow D_N$, with D_N the IR fixed point. As an example, see figure 1 illustrating the dRG flow for $N = 2$.

For $N \geq 6$ things are more intriguing. The operator $\hat{\mathcal{O}}_{S,-}$ becomes marginal when $\Delta = 0$. This suggests that $\hat{\mathcal{O}}_{S,-}$ is responsible for the flow between $D_p \rightarrow D_{N-p}$ ($p < N - p$), and it becomes marginal because the fixed points collide. Note that between $6 \leq N \leq 10$, we have symmetry breaking unitary defects for $p = 1$ and $p = N - 1$, and for the defect D_{N-1} the operator $\hat{\mathcal{O}}_{S,-}$ is *irrelevant*, so it corresponds to an IR fixed point of the dRG flow.

Finally, there are the defect operators $\hat{\mathcal{O}}_{T,\pm}$, which trigger dRG flows with an explicit symmetry breaking (e.g. the flow $D_0 \rightarrow D_1$ in figure 1). It's interesting to note that the symmetry preserving defect D_N contains the operator $\hat{\mathcal{O}}_{T,+}$ which becomes relevant for $N > 6$

$$\hat{\Delta}_{T,+} - 2 = -\frac{N-6}{N+8}\epsilon + \dots \quad (2.18)$$

This is easy to understand at large N . The dRG flow mixes the singlet and symmetric traceless representations of h_{ij} through the quadratic term $h_{ik}h_{kj} \sim (h_S^2 + \frac{1}{N}h_T^2)\delta_{ij} + \dots$ of the beta function (2.10). In the large N limit this interaction term vanishes and the representations decouple, leaving $\hat{\mathcal{O}}_{T,+}$ the symmetric traceless part of $[\varphi^i\varphi^j]$, which is a relevant operator.

Note that even though $\hat{\mathcal{O}}_{T,+}$ is a relevant operator in this case, it involves an explicit symmetry breaking so does not signal an instability of the fixed points.

The conformal manifold. An interesting feature of these symmetry breaking defects is the presence of a conformal manifold. Any choice of matrix h_{ij} with eigenvalues h_p and h_{N-p} as above defines an equivalent defect D_p (i.e. they are related by an $O(N)$ transformation). The space of such matrices is the Grassmanian

$$\mathbf{Gr}_p(N) = \frac{O(N)}{O(p) \times O(N-p)}, \quad (2.19)$$

which is interpreted as the conformal manifold for the dCFT. The breaking of symmetry implies the existence of local operators \mathbb{O}^{am} ($a = 1, \dots, p$ and $m = p+1, \dots, N$) in the dCFT which arise as contact terms for the broken $O(N)$ currents

$$\partial_{\mu} j^{\mu am}(x) D_p = D_p[\mathbb{O}^{am}(x_{\parallel})]\delta^{(d-2)}(x_{\perp}), \quad \mathbb{O}^{am} = (h_{p,+} + h_{N-p,-})M^{\epsilon}\varphi^a\varphi^m. \quad (2.20)$$

These operators—sometimes called tilt operators—are exactly marginal and generate translations on the conformal manifold. Because of their geometric interpretation, their correlators are constrained by integrated Ward identities [38] (see also [39]).

We note that the combination of eigenvalues appearing in the tilt operator has the simple expression

$$h_{p,+} + h_{N-p,-} = \frac{2(N+6)}{(N+8)}\pi\epsilon + \dots \quad (2.21)$$

2.3 General breaking of symmetries

One can also consider more general dRG flows, where we allow for the $O(N)$ symmetry to be broken to a subgroup $\prod_l O(p_l)$. It is a simple exercise to write and solve the beta functions for $l = 3$, which reveals that there is no new fixed point with 3 different eigenvalues h_l at this order in ϵ .

This follows from a simple counting argument. 3 quadratic equations can have at most 8 solutions, and all of them are already accounted for by degenerate cases where two eigenvalues coincide: In addition to the trivial solution $h = 0$ and the symmetry preserving defect $h_{p_1} = h_{p_2} = h_{p_3}$, there are 3 conditions for degeneracy ($h_1 = h_2$ and permutations) and in each case we have 2 nontrivial solutions. Therefore there cannot be new fixed points with $l = 3$ symmetry breaking at this order in perturbation theory, and by induction $l > 3$ can be excluded as well.

It would be interesting to see if subleading corrections to h lift the degeneracies and lead to defects with more complicated breakings of symmetry.

3 Large N expansion

To understand the fate of surface operators across dimensions and especially at $d = 3$, a convenient tool is the large N expansion. From the analysis near $d = 4$, we expect the symmetry preserving defects D_N to be the most relevant in the IR, so in this section we focus on these and show that they can be reliably studied away from $d = 4$.

The standard way to approach the large N limit of the $O(N)$ model is to use the Hubbard-Stratonovich transformation, see [40] for a review. Following [41], we rewrite the action (2.1) with an auxiliary field σ as

$$S = \int d^d x \left[\frac{1}{2} (\partial_\mu \varphi^i)^2 + \frac{1}{2\sqrt{N}} \sigma \varphi^i \varphi^i - \frac{3M^{d-4}}{2N\lambda} \sigma^2 \right]. \quad (3.1)$$

Upon integrating out σ one recovers the original action (2.1). At large N , the interaction term $\sigma \varphi^2$ promotes σ to a dynamical field by generating a effective propagator from an infinite sum of bubble diagrams (the solid black line is the propagator for σ and \bullet is the vertex $\sigma \varphi^2$)

$$\text{————} = \text{◀} \text{---} \text{◻} \text{---} \text{▶} + \text{◀} \text{---} \text{◻} \text{---} \text{◻} \text{---} \text{▶} + \dots \quad (3.2)$$

These diagrams assemble into a geometric series, and resumming one finds the effective propagator

$$\langle \sigma(x_1) \sigma(x_2) \rangle = \frac{C_\sigma}{|x_{12}|^{2\Delta_\sigma}}, \quad C_\sigma = \frac{2^{d+2} \Gamma\left(\frac{d-1}{2}\right) \sin\left(\frac{\pi d}{2}\right)}{\pi^{3/2} \Gamma\left(\frac{d}{2} - 2\right)} + O(N^{-1}). \quad (3.3)$$

The conformal dimension is $\Delta_\sigma = 2 + \gamma_\sigma$ with the anomalous dimension subleading in N at large N and given by

$$\gamma_\sigma = \frac{1}{N} \frac{4\Gamma(d) \sin\left(\frac{\pi d}{2}\right)}{\pi \Gamma\left(\frac{d}{2} + 1\right) \Gamma\left(\frac{d}{2} - 1\right)} + O(N^{-2}). \quad (3.4)$$

In the following we also need the 3-point function of σ obtained in [42–44]

$$\langle \sigma(x_1) \sigma(x_2) \sigma(x_3) \rangle = \frac{C_{\sigma\sigma\sigma}}{|x_{12}|^{\Delta_\sigma} |x_{13}|^{\Delta_\sigma} |x_{23}|^{\Delta_\sigma}}, \quad (3.5)$$

$$C_{\sigma\sigma\sigma} = -\frac{1}{\sqrt{N}} \frac{\Gamma\left(3 - \frac{d}{2}\right)}{\Gamma(d-3)} \left(\frac{2^{d-1} \Gamma\left(\frac{d-1}{2}\right) \sin\left(\frac{\pi d}{2}\right)}{\pi^{3/2}} \right)^3 + O(N^{-3/2}). \quad (3.6)$$

In this description, symmetry preserving defects are given by the integral of σ

$$D = \exp\left(-\int d^2\tau h\sigma(\tau)\right). \quad (3.7)$$

The beta function for the coupling h is given by (1.2). Solving for its zero we find the fixed point corresponding to the defect D_N for any d

$$\beta_h = \gamma_\sigma h + \pi C_{\sigma\sigma} h^2 + \dots, \quad \Rightarrow \quad h_* = -\frac{\gamma_\sigma}{C_{\sigma\sigma}\pi} + \dots. \quad (3.8)$$

The structure of the dRG flow is easy to understand and follows from the sign of the anomalous dimension γ_σ . When $2 < d < 4$, the anomalous dimension is negative $\gamma_\sigma < 0$, so the operator σ is marginally relevant and leads to a dRG flow from the trivial defect to D_N . The $O(N)$ model is still defined for $4 < d < 6$ [41] but in that case $\gamma_\sigma > 0$, so σ is a marginally irrelevant perturbation. The defect D_N may then be thought of as a UV fixed point of the dRG flow ending at the trivial defect.

A short calculation shows that the 1-point function of σ is given by

$$\langle\sigma(x)D\rangle = -h_* \int d^2\tau \langle\sigma(x)\sigma(\tau)\rangle + \dots = -\frac{\pi C_\sigma h_*}{x^2}. \quad (3.9)$$

The normalisation independent quantity associated to h_* is a_{φ^2} , which we obtain by dividing by the normalisation of σ (3.3) and comparing to (1.6)

$$a_{\varphi^2} = -\pi\sqrt{C_\sigma}h_* = -\frac{1}{\sqrt{N}} \frac{2^{1+\frac{d}{2}}(d-1)}{\pi^{\frac{3}{4}}d(d-3)} \sqrt{\frac{\Gamma\left(\frac{d-1}{2}\right)\sin\left(\frac{\pi d}{2}\right)}{\Gamma\left(\frac{d-4}{2}\right)}} + O(N^{-3/2}). \quad (3.10)$$

A plot of a_{φ^2} is presented in figure 2, and its values at integer dimensions are given in table 2. At dimensions $d = 2, 4, 6$, it has zeros because the anomalous dimension γ_σ (3.4) vanishes at large N for even integer dimensions. In particular near $d = 4$, it behaves as $-|\epsilon|$ since both γ_σ and $C_{\sigma\sigma\sigma}$ change sign, and the coefficient matches with the large N limit of the result from the ϵ -expansion (2.13) as expected.

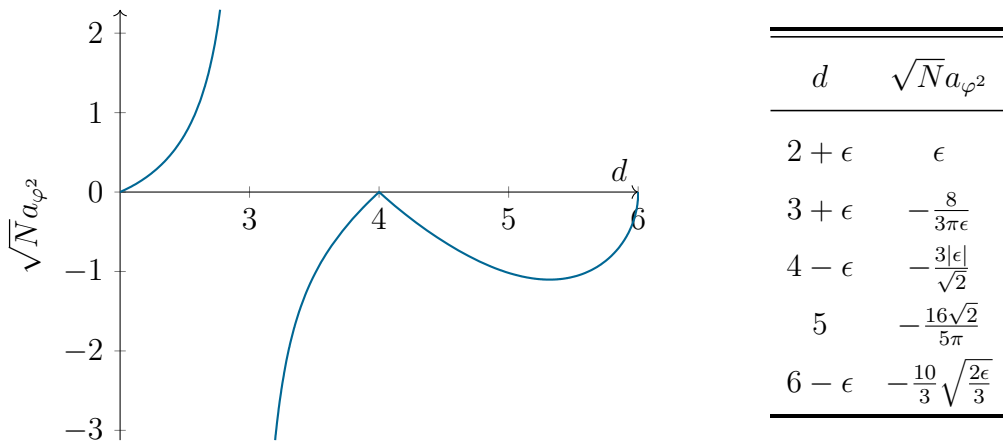


Figure 2: On the left, a plot of $a_{\varphi^2}(d)$ to leading order at large N . On the right, the corresponding values near integer dimensions.

An interesting feature is the divergence at $d = 3$, which follows from the vanishing of the structure constant $C_{\sigma\sigma\sigma}$ at large N [42–44]. This signals a breakdown of the small h_* approximation leading to further corrections of the beta function (3.8). We discuss two cases.

The first possibility is that the zero of the beta function becomes of order $O(N^0)$. The leading contribution to the renormalisation of the coupling h comes from the diagram

$$\text{Diagram} \sim \int_{\mathbb{R}^2} d^2\tau_{1,2,3} \langle \sigma(x)\sigma(\tau_1)\sigma(\tau_2)\sigma(\tau_3) \rangle_{\text{connected}} \sim \frac{h^3}{N} \frac{A}{x^2} + \dots \quad (3.11)$$

for some A . If A is nonzero and the diagram contributes to the beta function, then we expect $\beta \sim \gamma_\sigma h + \frac{Bh^3}{N} + \dots = 0$ for some B , and since $\gamma_\sigma \sim N^{-1}$ we would find two nontrivial fixed points $h_* \sim O(N^0)$.

Doing this calculation explicitly seems difficult because the 4-point function of σ is only known partially at large N [45]. However one might suspect that the fixed points are absent ($B = 0$) for two reasons. First, there have been explicit studies of boundary/interface fixed points at low values of N (e.g. [46, 47, 14]) with no indications of such new fixed points. Second, a simpler version of this question is to restrict to $d = 4 - \epsilon$, where the Feynman diagrams can be evaluated more easily. This is presented in appendix A.2 and we verify that $B|_{d=4-\epsilon} = 0$, which suggests that perhaps also $B|_{d=3} = 0$.

The second possibility is that the zero of the beta function becomes of order \sqrt{N} . In this regime the behavior of the fixed points is well-understood from the large N analysis of [1, 2, 4, 21, 12] for an interface in $d = 3$. There are two symmetry preserving fixed points, known in the literature as the special and ordinary transitions. The special transition corresponds to the trivial interface and is characterised by $a_{\varphi^2, sp} = 0$. The ordinary transition on the other hand is a nontrivial interface and is characterised by [4]

$$a_{\varphi^2, ord} = -\frac{\pi\sqrt{N}}{8} + O(N^{-1/2}). \quad (3.12)$$

Therefore I expect that the divergence of a_{φ^2} at $d = 3$ should be interpreted as a change in scaling with respect to N , and that D_N becomes the ordinary fixed point.

Finally, note that there is a third fixed point known as the extraordinary (or normal) transition. That interface is characterised by a nonzero one-point function for φ^i breaking the $O(N)$ symmetry down to $O(N - 1)$. Below $d = 3$, a_{φ^2} becomes positive (or equivalently $h_* < 0$), which can be interpreted as sourcing a negative mass for φ^2 . This signals an instability at $\phi^i = 0$, and including a defect coupling $u^i \phi^i$ in (3.7), we expect the stable IR fixed point to have nonzero u^i , leading to the extraordinary fixed point.

4 ϵ -expansion in $d = 6 - \epsilon$

The critical $O(N)$ model can be analytically continued to the range $4 < d < 6$, where it is described by the (perturbative) UV fixed point of the action (2.1). It can be studied using an ϵ -expansion at $d = 6 - \epsilon$ from the action [41]

$$S = \int d^{6-\epsilon}x \left[\frac{1}{2}(\partial_\mu \varphi^i)^2 + \frac{1}{2}(\partial_\mu \sigma)^2 + \frac{M^{\frac{\epsilon}{2}} g_1}{2} \sigma \varphi^i \varphi^i + \frac{M^{\frac{\epsilon}{2}} g_2}{6} \sigma^3 \right]. \quad (4.1)$$

This theory is conformal when setting the coupling constants to their critical values g_1^*, g_2^* , which have been calculated in [41]⁴ (see also [48–51] for subleading corrections up to $O(\epsilon^5)$)

$$\begin{aligned} g_1^* &= \sqrt{\frac{6(4\pi)^3\epsilon}{N}} \left(1 + \frac{22}{N} + \frac{726}{N^2} - \frac{326180}{N^3} + \dots \right), \\ g_2^* &= \sqrt{\frac{6(4\pi)^3\epsilon}{N}} \left(6 + \frac{972}{N} + \frac{412596}{N^2} + \frac{247346520}{N^3} + \dots \right). \end{aligned} \quad (4.2)$$

In this section we study surface operators in the $d = 6 - \epsilon$ description. Doing so provides another nontrivial check of the large N results obtained in section 3. Perhaps more importantly, because the dimension of a free scalar field is $\Delta_\varphi = 2$ in $d = 6$, we can reliably study dRG flows of surface operators with a coupling to φ^i using perturbation theory

$$D = \exp \left[- \int d^2\tau \left(h\sigma + u^i \varphi^i \right) \right]. \quad (4.3)$$

When $u \neq 0$ these surface operators preserve an $O(N - 1)$ symmetry and are relevant for describing the extraordinary transition in $d = 3$.

Unlike our treatment in section 2, here to any order in g_1 and g_2 the number of Feynman diagrams contributing to the renormalisation of the defect is finite, and we can treat h, u nonperturbatively (this is similar to [20]). The beta functions for the defect couplings involve a term linear in ϵ from the classical dimension of the fields, so for consistency one should calculate the beta functions to order $g^2 \sim \epsilon$. The diagrams contributing to that order can be found in tables 3 and 4. A straightforward calculation detailed in appendix A.3 leads to the beta functions

$$\begin{aligned} \beta_h &= (\Delta_\sigma - 2) h - \frac{g_1 u^2 + g_2 h^2}{(4\pi)^2} - \frac{2g_1^2 h u^2 + g_1 g_2 h u^2 + g_2^2 h^3}{(4\pi)^4} + \dots \\ \beta_{u^i} &= (\Delta_\varphi - 2) u^i - \frac{2g_1 h u^i}{(4\pi)^2} - \frac{g_1(2g_1 h^2 + g_1 u^2 + g_2 h^2) u^i}{(4\pi)^4} + \dots \end{aligned} \quad (4.4)$$

where the conformal dimensions are [41]

$$\Delta_\sigma = 2 - \frac{\epsilon}{2} + \frac{1}{(4\pi)^3} \frac{N g_1^2 + g_2^2}{12} + O(g^4) = 2 + \left(\frac{40}{N} + \frac{6800}{N^2} + \dots \right) \epsilon + O(\epsilon^2), \quad (4.5)$$

$$\Delta_\varphi = 2 - \frac{\epsilon}{2} + \frac{g_1^2}{6(4\pi)^3} + O(g^4) = 2 + \left(-\frac{1}{2} + \frac{1}{N} + \frac{44}{N^2} + \frac{1936}{N^3} + \dots \right) \epsilon + O(\epsilon^2). \quad (4.6)$$

The terms linear and quadratic in h, u match the general form (1.2), and in addition we have terms cubic in h, u and quadratic in g .

The simplest fixed point is the trivial defect with $h = u = 0$. Below we analyse the fixed points describing the symmetry preserving defect D_N as well as symmetry breaking defects.

Note that similar dRG flows were considered in [52–54]. Their analysis involves a double-scaling limit where the bulk theory is not critical such that diagrams contributing to the anomalous dimension of φ, σ are suppressed.

⁴These are asymptotic series at large N . The behavior of the fixed point at finite N is discussed in [41].

4.1 Symmetry preserving defect

Setting $u = 0$, the beta function for h factorises. There are 3 solutions, $h = 0$ and two nontrivial fixed points at

$$h_* = -\frac{8\pi^2}{g_2} \left(1 \pm \sqrt{1 + 4(\Delta_\sigma - 2)} \right). \quad (4.7)$$

The simpler fixed point to analyse is the negative root, which is a perturbative fixed point analogous to those of sections 2 and 3. We find

$$h_* = \frac{16\pi^2}{g_2} (\Delta_\sigma - 2) = \frac{20}{3} \sqrt{\frac{2\pi\epsilon}{3N}} \left(1 + \frac{8}{N} - \frac{4118}{N^2} + \dots \right). \quad (4.8)$$

This describes the symmetry preserving defect D_N , as can be shown by comparing the value of a_φ^2 to the large N result. A short calculation of the 1-point function of σ (see table 3) allows us to extract

$$a_\varphi^2 = -\frac{10}{3} \sqrt{\frac{2\epsilon}{3N}} \left(1 + \frac{8}{N} - \frac{4118}{N^2} + \dots \right), \quad (4.9)$$

which agrees with the leading large N result (3.10), see figure 2.

Since σ is an irrelevant defect operator ($\Delta_\sigma > 2$) at the trivial defect, one should interpret (4.8) as a UV fixed point for a dRG flow. Indeed, we can check that $\hat{\sigma}$ is marginally relevant at the fixed point

$$\hat{\Delta}_\sigma = 2 + \beta'(h)|_{h_*} = 2 - \left(\frac{40}{N} + \frac{6800}{N^2} + \dots \right) \epsilon + O(\epsilon^2). \quad (4.10)$$

The fixed point at the positive root of (4.7) is more subtle. We have $h_* \sim g_2^{-1}$ for a large negative value of h_* . Since the combination $h_* g_* \sim O(\epsilon^0)$ is not a small parameter, the beta function may receive additional contributions and the validity of the solution cannot be established in our approximation. One may expect that it disappears when including subleading corrections to the beta function (4.4). For instance, when using the Padé approximant

$$\beta_h \supset -\frac{g_2 h^2}{(4\pi)^2} - \frac{g_2^2 h^3}{(4\pi)^4} + \dots \sim -\frac{h}{1 - \frac{g_2 h}{(4\pi)^2}}, \quad (4.11)$$

the beta function only has the fixed points $h = 0$ and (4.8).

4.2 Symmetry breaking defect

We now turn to solutions with $u \neq 0$, which breaks the $O(N)$ symmetry to $O(N-1)$. It's convenient to write $u^i = u n^i$, with n^i a unit length vector parametrising the symmetry breaking. For nonzero u there are 3 solutions to the beta functions, and only one can be studied reliably using perturbation theory (the other two have $h_*, u_* \sim \sqrt{N/\epsilon}$ with $h_* < 0$). Taking $h_*, u_* \sim \sqrt{\epsilon}$ as an ansatz, it is easy to solve the beta functions to find

$$h_* = \frac{\Delta_\varphi - 2}{2\tilde{g}_1} + O(\epsilon^{3/2}), \quad (4.12)$$

$$u_*^2 = \frac{\pi^2(\tilde{g}_1^2 - \frac{3\epsilon}{4\pi})(N\tilde{g}_1^3 + \tilde{g}_1\tilde{g}_2^2 - \tilde{g}_1^2\tilde{g}_2 + (\tilde{g}_2 - 2\tilde{g}_1)\frac{3\epsilon}{4\pi})}{9\tilde{g}_1^3} + O(\epsilon^{3/2}). \quad (4.13)$$

Plugging in the value of g (4.2) we get

$$h_* = -\frac{1}{2}\sqrt{\frac{\pi\epsilon}{6N}} \left[1 - \frac{24}{N} - \frac{286}{N^2} + \frac{346024}{N^3} + \dots \right], \quad (4.14)$$

$$u_*^2 = -\frac{\pi N \epsilon}{12} \left[3 + \frac{356}{N} + \frac{184652}{N^2} + \frac{117474208}{N^3} + \dots \right]. \quad (4.15)$$

u_*^2 is negative since $\tilde{g}_1^2 < \frac{3\epsilon}{4\pi}$. This is clear from the asymptotic expression at large N and can be checked for finite $N \gtrsim 1038.27$ using the expressions for g given in [48]. The solution is then a complex fixed point which corresponds to a nonunitary dCFT. As already mentioned in section 2.2, such fixed points are not reached by unitary dRG flows.

Note that $u_* \sim \sqrt{N}$ has the correct scaling to describe the normal transition in $d = 3$. I report here the eigenvalues of the jacobian at the fixed points

$$\epsilon \left[\frac{3 \pm \sqrt{3}}{2} + \frac{227 \pm \frac{437}{\sqrt{3}}}{N} + \frac{100288 \pm \frac{557024}{3\sqrt{2}}}{N^2} + \dots \right]. \quad (4.16)$$

Both of these are real and positive. In addition to these operators, the dCFT contains a tilt operator $\mathbb{O}^i = u_* \varphi^i$ associated to the breaking of symmetry $O(N) \rightarrow O(N-1)$. Since u_* is imaginary, these operators have negative norm.

5 The anomaly coefficients

Having obtained the fixed points describing conformal surface operators in the previous sections, I now turn to the calculation of their anomaly coefficients (1.3). Anomaly coefficients have been studied in the past in many contexts, and it turns out that most of the results we need are already known. The coefficient a for a surface operator of the form (1.1) was obtained in [25, 19] using conformal perturbation theory, and their calculation can be applied to our defects as well, with the exception of $d = 3$ where conformal perturbation theory no longer applies (in $d = 3$ however the coefficient a was obtained independently in [21, 12]). The rest of the coefficients were calculated previously for surfaces in 6d [55, 56, 23], and as I discuss below their calculation can be extended to surfaces in arbitrary dimensions as well.

Surface in $d = 6 - \epsilon$. The simplest case to consider is surfaces in 6d, which couple directly to the scalar fields σ and φ^i as in (4.3). Their conformal anomaly can be obtained by calculating the expectation value of a surface operator over the arbitrary surface $\Sigma \subset \mathbb{R}^{6-\epsilon}$ and placing the theory on a curved background of metric G . In perturbation theory, the leading contribution to their conformal anomaly is given by an integrated propagator of the form

$$\frac{1}{2} \int_{\Sigma} \text{vol}_{\Sigma}(\tau_1) \text{vol}_{\Sigma}(\tau_2) u^i(\tau_1) u^j(\tau_2) \langle \varphi^i(\tau_1) \varphi^j(\tau_2) \rangle_G + O(u^3), \quad (5.1)$$

and we're interested in the $\log \tilde{\epsilon}$ divergences of that integral, where $\tilde{\epsilon}$ is a UV cutoff. These divergences come from coincident points $\tau_1 \rightarrow \tau_2$ and obey the structure of a conformal anomaly (1.3). They can be calculated from the small distance expansion of the curved

space propagator for a conformal scalar in 6d, which reads [56] (in normal coordinates about the origin)

$$\langle \varphi^i(0)\varphi^j(\xi) \rangle_G = \frac{C_{d,1}\delta^{ij}}{|\xi|^4} \left[1 + \frac{1}{3}P_{\mu\nu}\xi^\mu\xi^\nu + \dots \right], \quad (5.2)$$

with $C_{d,1}$ the canonical normalisation for a scalar field in d dimensions defined in (A.3) and $P_{\mu\nu} = \frac{1}{d-2} \left(R_{\mu\nu} - \frac{2}{d-1}RG_{\mu\nu} \right)$ is the Schouten tensor.

The corresponding anomaly coefficients were obtained in [55, 56, 23] and are given by

$$a = 0, \quad b_1 = -\frac{\pi^2 C_{d,1} u^2}{2}, \quad b_2 = \frac{\pi^2 C_{d,1} u^2}{3}, \quad c = \pi^2 C_{d,1} u^2. \quad (5.3)$$

The vanishing of a to leading order has a simple explanation: the coefficient a measures the conformal anomaly associated to a change in topology from the plane to the sphere, which is zero because the 2-point function of a (conformal) scalar appearing in the integrand of (5.1) is conformally invariant.⁵

For a surface operator obtained by integrating $u_i \mathcal{O}^i$ as in (1.1), [25, 19] shows that the leading contribution to a instead comes at order $O(\epsilon u^2)$ and is given by

$$a = \frac{\pi^2}{6} (\Delta_{\mathcal{O}} - 2) C_{\mathcal{O}} u^2 + O(u^4), \quad (5.4)$$

where $C_{\mathcal{O}}$ is the normalisation constant appearing in the 2-point function of \mathcal{O} .

From these results we can read the anomaly coefficients for surfaces defects (4.3) at $d = 6 - \epsilon$. Adding the contribution of each scalar, we get to leading order,

$$a = \frac{(\Delta_{\sigma} - 2)h_*^2 + (\Delta_{\varphi} - 2)u_*^2}{24\pi}, \quad b_1 = -\frac{h_*^2 + u_*^2}{8\pi}, \quad b_2 = \frac{h_*^2 + u_*^2}{12\pi}, \quad c = \frac{u_*^2}{4\pi}, \quad (5.5)$$

where the conformal dimensions are given in (4.6) and the values of the fixed points are respectively in (4.8) and (4.15) for the symmetry preserving and breaking defects. We note that the contribution from the symmetry breaking term in (1.3) is here $(\partial n)^2 = \partial_a n^i \partial_b n^i h^{ab}$ with h_{ab} the induced metric on Σ and n^i is the unit vector parallel to u^i .

Focussing on the symmetry preserving defect D_N (4.8), the anomaly coefficients are

$$a = \frac{4000\epsilon^2}{81N^2} \left(1 + \frac{186}{N} + \frac{60492}{N^2} + \dots \right), \quad b_1 = -\frac{3b_2}{2} = -\frac{100\epsilon}{27N} \left(1 + \frac{16}{N} - \frac{8172}{N^2} + \dots \right). \quad (5.6)$$

The coefficient a is positive in accordance with the a -theorem (1.4) if we interpret these defects as UV fixed points of the dRG flow ending at the trivial defect.

Surface in $d = 4 - \epsilon$. The previous calculation of the anomaly coefficients relies on the small distance expansion of the 2-point function (5.2), which is known in 6d. Its generalisation to d dimensions requires the 2-point function for an operator \mathcal{O}^I of dimension 2 in a d dimensional CFT. Requiring that it reduces to the usual 2-point function when the metric is flat sets

$$\langle \mathcal{O}^I(0)\mathcal{O}^J(\xi) \rangle_g = \frac{C_{\mathcal{O}}\delta^{IJ}}{|\xi|^{2\Delta_{\mathcal{O}}}} [1 + (\alpha R_{\mu\nu} + \beta Rg_{\mu\nu})\xi^\mu\xi^\nu + \dots], \quad (5.7)$$

⁵This is no longer true if the operators have anomalous dimensions, in which case the coefficient receives subleading contributions.

with α, β constants that could a priori depend on d and $\Delta_{\mathcal{O}}$. One can check that the UV divergences calculated as in [55, 56, 23] respect the structure of a conformal anomaly (1.3) only when $R_{\mu\nu}$ and R assemble into the Schouten tensor $P_{\mu\nu}$ with coefficient $1/3$. Therefore we conclude that by consistency, the correlator must take the same form as the propagator for scalars in 6d (5.2) and the previous calculation extends to any dimension d .

For the symmetry preserving defect (2.11), we use (5.4) and (5.3) to get

$$a = -\frac{9N\epsilon^3}{2(N+8)^3}, \quad b_1 = -\frac{9N\epsilon^2}{4(N+8)^2}, \quad b_2 = \frac{3N\epsilon^2}{2(N+8)^2}. \quad (5.8)$$

For the symmetry breaking defect (2.17), there is a contribution to the anomaly from the symmetry breaking term $(\partial n)^2 = \partial_a n^{ij} \partial_b n^{ij} h^{ab}$, where h_{ab} is the induced metric on Σ and n^{ij} is the unit norm tensor parallel to h^{ij} . The anomaly coefficients b_1, b_2, c are straightforward to obtain and given by

$$b_1 = -\frac{c}{2}, \quad b_2 = \frac{c}{3}, \quad (5.9)$$

along with

$$\begin{aligned} c &= \frac{h^{ij} h^{ij}}{64\pi^2} = \frac{ph_{p,+}^2 + (N-p)h_{N-p,-}^2}{16\pi^2} \\ &= \frac{3\epsilon^2}{8(N+8)^2} (3N + 2p(N-p) + (N-2p)\Delta). \end{aligned} \quad (5.10)$$

Note that when $p = N$, $c \neq 0$ but $(\partial n)^2 = 0$, so we recover the result (5.8).

For the coefficient a , we need to treat separately each irreducible representation to get

$$a = \frac{\pi^2}{6} (\Delta_{\varphi_S^2} - 2) C_{\varphi_S^2} \frac{(h_{ii})^2}{4} + \frac{\pi^2}{6} (\Delta_{\varphi_T^2} - 2) (C_{\varphi_T^2})_{ijkl} \frac{h^{ij} h^{kl}}{4}. \quad (5.11)$$

The coefficient $C_{\varphi_T^2}$ can be read from the 2-point function of φ_T^2 . Plugging in the conformal dimensions along with the values of h , we find

$$a = \frac{\epsilon^3}{48(N+8)^3} \left[8\Delta^4 + 4(N-2p)\Delta^3 + (N+6)(N-6)\Delta^2 - 9(N+6)^2 \right]. \quad (5.12)$$

For any $N \leq 6$ and $0 \leq p \leq N$, we can check that $\Delta > 0$ and a satisfies

$$a_{p=0} \geq a_{p=1} \geq \dots \geq a_{p=N}. \quad (5.13)$$

This has a direct implication for defect RG flows. For any given N , one can consider dRG flows between symmetry breaking surface defects D_p and $D_{p'}$. Because of the a -theorem $a_{UV} > a_{IR}$ [25], we conclude that dRG flows can only increase p , so that $p' > p$. We then expect a sequence of dRG flows that interpolate between defects of increasing p

$$D_0 \rightarrow D_1 \rightarrow \dots \rightarrow D_N, \quad (5.14)$$

with a concrete example being the flow $D_0 \rightarrow D_1 \rightarrow D_2$ presented in figure 1. It would be interesting to check if this structure is preserved at higher orders in the ϵ -expansion.

Large N . Finally we can calculate the anomaly coefficients at large N as well. Using (5.4) and (5.3) we get

$$a = \frac{C_\sigma^3 \gamma_\sigma^3}{6C_{\sigma\sigma\sigma}^2}, \quad b_1 = -\frac{C_\sigma^3 \gamma_\sigma^2}{2C_{\sigma\sigma\sigma}^2}, \quad b_2 = \frac{C_\sigma^3 \gamma_\sigma^2}{3C_{\sigma\sigma\sigma}^2}, \quad c = 0, \quad (5.15)$$

where $C_{\sigma\sigma\sigma}$ is given in (3.6), γ_σ in (3.4) and C_σ in (3.3). Plugging in the values we get

$$a = \frac{1}{N^2} \frac{(d-2)(d-1)d^2}{3(d-3)^2} \frac{\Gamma(d)^2 \operatorname{sinc}\left(\frac{\pi d}{2}\right)}{\Gamma\left(\frac{d-4}{2}\right) \Gamma\left(\frac{d+2}{2}\right)^3}, \quad (5.16)$$

and

$$\frac{C_\sigma^3 \gamma_\sigma^2}{C_{\sigma\sigma\sigma}^2} = \frac{1}{N} \frac{(d-4)(d-2)(d-1)}{2(d-3)^2} \frac{\Gamma(d) \operatorname{sinc}\left(\frac{\pi d}{2}\right)}{\Gamma\left(\frac{d+2}{2}\right)}. \quad (5.17)$$

Setting $d = 4 - \epsilon$ and $d = 6 - \epsilon$ we recover the large N limit of the anomaly coefficients (5.8) and (5.6) as expected. Also notice that $a < 0$ when $2 < d < 4$ and $a > 0$ when $4 < d < 6$, in accordance with the a -theorem.

5.1 The string potential

Given two planar surface defects separated a distance L , it is well-known that quantum fluctuations can generate a potential $\frac{U_0 \text{Area}}{L^2}$. A generalisation of this observable called the (generalised) string potential was introduced in [31] and is related to the anomaly coefficient b_1 , at least to leading order in the small perturbative parameter (ϵ or N^{-1}).

Consider the surface consisting of two hemispheres inside an S^3 of radius R and glued along their boundary at an angle $\pi - \phi$. Using $u \in [0, \pi/2]$, $v \in [0, 2\pi)$ each hemisphere can be parametrised by

$$\begin{aligned} x^1 &= R \cos u \cos v, & x^2 &= R \cos u \sin v, \\ x^3 &= R \sin u \cos w, & x^4 &= R \sin u \sin w, \end{aligned} \quad (5.18)$$

for a fixed w , and we take respectively $w = \phi/2$ and $w = \pi - \phi/2$ for each hemisphere. When $\phi = 0$, this is the geometry of a sphere, while in the limit $\phi \rightarrow \pi$ the two hemispheres become superimposed. As shown in [31] the expectation value of a surface defect D_ϕ with this geometry defines a potential $U(\phi)$ through

$$U(\phi) = \frac{1}{2\pi} \left(\log \langle D_\phi \rangle - \log \langle D_{\phi=0} \rangle \right). \quad (5.19)$$

This definition is easy to motivate. The defect D_ϕ is topologically a sphere, so it has a conformal anomaly and its expectation value is ill-defined. However the anomaly cancels exactly in the ratio between the expectation values at any two angles (here ϕ and 0), leading to a well-defined quantity. The factor 2π is simply the area of the hemisphere, so that U calculates a potential density.

The expectation value of D_ϕ can be calculated in terms of an integrated 2-point function of the form (5.1) and yields, to leading order [31],

$$U(\phi) = \frac{b_1}{2\pi \cos(\phi/2)^2} + \dots \quad (5.20)$$

In particular, setting $\phi = \pi - \delta$ and taking the limit $\delta \rightarrow 0$ we get

$$U(\pi - \delta) = \frac{2b_1}{\pi\delta^2} + \dots \quad (5.21)$$

This can be interpreted as $\frac{U_0}{L^2}$ with the identification $L = \delta$. Note that U_0 is negative, so the force between the defects is attractive, as expected for a force mediated by a scalar field. Up to a different value for h_* , this agrees with the result of [52].

It would be interesting to determine whether the relation to the anomaly coefficients still holds at subleading orders.

6 Discussion

Surface defects are ubiquitous objects in CFTs, and have been mostly studied in the context of gauge theories where they play a fundamental role (e.g. in 4d $\mathcal{N} = 4$ SYM [57] and in the 6d $\mathcal{N} = (2, 0)$ theories [56, 23]). The present analysis shows that even in the simplest example of an interacting CFT there is an interesting array of surface defects. Thanks to this simplicity, one can perform perturbative calculations in overlapping regimes of validity, track dRG flows, study their fixed points and provide new nontrivial examples of the defect a -theorem.

The results obtained here suggest an interesting structure of fixed points across dimensions and upon varying N . The simplest defect to access is the symmetry preserving defect D_N , which seems to exist for $d \geq 3$ and any N . The most interesting case is $d = 3$, where the perturbative analysis breaks down and the coupling to φ^2 changes scaling with respect to N . I interpret this as evidence that D_N matches with the fixed point of the ordinary transition, but I haven't proven it. It would be interesting to confirm this expectation by extending the large N methods of [21] to subleading order in N and to surface defects in arbitrary dimensions.

Two related questions that I haven't attempted to address here are diagnosing the nature of two instabilities in the dRG flows. When $d < 4$, the trivial defect is unstable. In this paper I discuss flows with $h > 0$ ending at D_N , but as apparent in figure 1, dRG flows with $h < 0$ seem to belong to a different universality class, and interpreting $h < 0$ as a negative mass term, we expect spontaneous symmetry breaking leading to the extraordinary fixed point (i.e. where $\langle \varphi^i \rangle \neq 0$). When $d > 4$, the direction of the flow is reversed and the defect D_N becomes unstable. Turning on the defect operator $\hat{\sigma}$ with one sign leads to the trivial defect and is discussed in sections 3 and 4. With the other sign, it flows towards $h \rightarrow \infty$. That instability may be related to the unbounded potential for σ in (4.1).

In addition to D_N , the theory contains many instances of symmetry breaking defects. At $d = 6 - \epsilon$ I find a (nonunitary) fixed point (4.15) that may correspond to the extraordinary fixed point. Away from $\epsilon \ll 1$ the fixed point cannot be studied reliably using the present methods, but is expected to exist for any $2 < d < 6$ and any N . It would be interesting to study this fixed point using large N methods, and clarify whether there are additional nonperturbative fixed points with $h, u \sim \sqrt{N}$ as suggested by the perturbative beta functions (4.4).

As one lowers d , more defect operators become relevant and the structure of the fixed points becomes more intricate. Below $d = 4$, one may include a coupling to $\varphi^i \varphi^j$, which leads to symmetry breaking defects preserving $O(p) \times O(N - p) \subset O(N)$. Their behavior is

dictated by the sign of the discriminant Δ^2 (2.17). It would be interesting to understand the behavior of Δ as we vary d , especially whether these fixed points still exist for some $N \leq N_c$ at $d = 3$. More generally, I expect that a full characterisation of fixed points near $d = 3$ would involve also the coupling to φ^i as well as cubic and quartic terms in φ , and it would be interesting to include these terms in the analysis.

Although the focus of this paper is the critical $O(N)$ model, many more examples of vector models where the $O(N)$ symmetry is reduced to a subgroup were constructed in the ϵ expansion [58–60]. A systematic study of surface defects in these models (as well as generalisations involving complex scalars and fermions) as initiated in [61] for line defects is within reach and would expose an even richer spectrum of surface defects.

Finally, the 3d (5d) critical $O(N)$ model is expected to be dual to a higher spin theory on AdS_4 [62] (AdS_6), and it would be interesting to study the realisation of surface operators there.

Acknowledgements

It is a pleasure to thank Nadav Drukker, Zohar Komargodski, Diego Rodriguez-Gomez, Ritam Sihna, Andy Stergiou, Volodia Schaub and Yifan Wang for stimulating discussions. Special thanks go to N. Drukker and A. Stergiou for their helpful guidance, thoughtful comments on the preliminary version of this manuscript and many suggestions. I also want to thank M. Probst and D. Rodriguez-Gomez for sharing their notes on related topics with me.

A Explicit calculations

This appendix presents the derivation of the beta functions governing the renormalisation of the defect couplings for the surface operators introduced in (2.3) and (4.3). I calculate the relevant diagrams, with the results tabulated in tables 2, 3 and 4, from which I read the corresponding counterterms. The derivation of the beta function in $d = 4 - \epsilon$ is presented in section 2, and in section A.3 I present a more explicit derivation of the beta function in $d = 6 - \epsilon$.

A.1 Evaluating Feynman diagrams

Many of the Feynman diagrams we need are reducible to products of 1-loop diagrams, and can be evaluated easily in momentum space by using the identity (see e.g. [35])

$$\int \frac{d^d k}{(2\pi)^d} \frac{1}{(k^2)^a [(k-p)^2]^b} = \frac{1}{(p^2)^{a+b-d/2}} L_d^{(a,b)}, \quad (\text{A.1})$$

where we defined

$$L_d^{(a,b)} = \frac{\Gamma\left(\frac{d}{2} - a\right) \Gamma\left(\frac{d}{2} - b\right) \Gamma\left(a + b - \frac{d}{2}\right)}{(4\pi)^{d/2} \Gamma(a) \Gamma(b) \Gamma(d - a - b)}. \quad (\text{A.2})$$

To revert back to position space we use the Fourier transform

$$\int \frac{d^d p}{(2\pi)^d} \frac{e^{ipx}}{(p^2)^\alpha} = C_{d,\alpha} \frac{1}{(x^2)^{\frac{d}{2} - \alpha}}, \quad C_{d,\alpha} \equiv \frac{\Gamma\left(\frac{d}{2} - \alpha\right)}{4^\alpha \pi^{d/2} \Gamma(\alpha)}. \quad (\text{A.3})$$

As an example, we evaluate the diagram 2.4. Up to a prefactor, this is given by the integral of (two copies of) the propagator $G(x; y)$

$$M^{2\epsilon} \int d^2\tau G(x; \tau)^2, \quad (\text{A.4})$$

with the factor $M^{2\epsilon}$ ensuring that the integral is dimensionless. The momentum space representation of the propagator is given as usual by (this is the $\alpha = 1$ case of (A.3))

$$G(x; y) \equiv \frac{C_{d,1}}{|x-y|^{d-2}} = \int \frac{d^d p}{(2\pi)^d} \frac{e^{ip(x-y)}}{p^2}. \quad (\text{A.5})$$

Performing the τ integral and using (A.1) leaves us with

$$M^{2\epsilon} \int \frac{d^{d-2}p}{(2\pi)^{d-2}} \frac{d^d p'}{(2\pi)^d} \frac{e^{ipx}}{p'^2(p-p')^2} = M^{2\epsilon} \int \frac{d^{2-\epsilon}p}{(2\pi)^{2-\epsilon}} \frac{e^{ipx}}{p^\epsilon} L_{4-\epsilon}^{(1,1)} = \frac{(xM)^{2\epsilon}}{x^2} C_{2-\epsilon, \frac{\epsilon}{2}} L_{4-\epsilon}^{(1,1)}. \quad (\text{A.6})$$

Using these identities we can evaluate most of the diagrams entering the perturbative calculations in 4d, 6d and at large N . One exception is the diagram 2.6, which we analyse below.

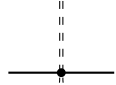
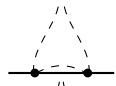
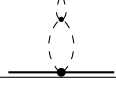
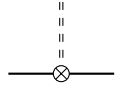
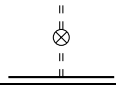
Diagram	Prefactor	Integral	ϵ -expansion
	$-h_{ij}$	$\frac{(xM)^{2\epsilon}}{x^2} C_{2-\epsilon, \frac{\epsilon}{2}} L_{4-\epsilon}^{(1,1)}$	$\frac{1}{16\pi^3 x^2} + \dots$
	$h_{ik} h_{kj}$	$\frac{(xM)^{3\epsilon}}{x^2} C_{4-\epsilon, 1} T_1$	$\frac{1}{32\pi^4 x^2 \epsilon} + \dots$
	$\frac{\lambda}{2} \frac{h_{KK} \delta_{ij} + 2h_{ij}}{3}$	$\frac{(xM)^{3\epsilon}}{x^2} C_{2-\epsilon, \epsilon} (L_{4-\epsilon}^{(1,1)})^2$	$\frac{1}{64\pi^5 x^2 \epsilon} + \dots$
	$-\delta h_{ij}$	$\frac{(xM)^{2\epsilon}}{x^2} C_{2-\epsilon, \frac{\epsilon}{2}} L_{4-\epsilon}^{(1,1)}$	$\frac{1}{16\pi^3 x^2} + \dots$
	$\delta_{\varphi_R^2} h_{ij}$	$\frac{(xM)^{2\epsilon}}{x^2} C_{2-\epsilon, \frac{\epsilon}{2}} L_{4-\epsilon}^{(1,1)}$	$\frac{1}{16\pi^3 x^2} + \dots$

Table 2: Feynman diagrams contributing to the renormalisation of h_{ij} to order $O(\lambda^2, \lambda h^2, h^3)$. We list the value of the integral of the propagators, its leading pole in the ϵ -expansion, and the overall prefactor of the integral. The values for $C_{d,\alpha}$ and $L_d^{(a,b)}$ are respectively given in (A.3) and (A.2). The counterterm $\delta_{\varphi_R^2}$ is defined in (2.7).

Diagram 2.6. It is useful to consider the more general integral

$$M^{(m+2)\epsilon} \int d^2\tau_1 d^2\tau_2 \frac{C_{d,1}^3}{|x-\tau_1|^{2-\epsilon} |\tau_1-\tau_2|^{2-m\epsilon} |x-\tau_2|^{2-\epsilon}}. \quad (\text{A.7})$$

When $m = 1$, this reduces to the diagram 2.6. Using either momentum or position space propagators, one can reduce this to the integral over Feynman parameters

$$\frac{(xM)^{(m+2)\epsilon}}{x^2} C_{d,1} T_m, \quad (\text{A.8})$$

where we defined

$$T_m = \frac{\Gamma\left(1 - \frac{(m+2)\epsilon}{2}\right)}{16\pi^{2-\epsilon}\Gamma\left(1 - \frac{m\epsilon}{2}\right)} \int_0^1 du \int_0^1 dv u^{-1+\frac{m\epsilon}{2}} v^{-\frac{\epsilon}{2}} [(1-u)(1-v)]^{-\frac{(m+1)\epsilon}{2}} (1-uv)^{-1+\frac{(m+2)\epsilon}{2}}. \quad (\text{A.9})$$

This integral is easy to do by expanding $(1-uv)^{-1+\frac{(m+2)\epsilon}{2}}$ in series, in which case the integral factorises into two beta functions to give

$$\frac{\Gamma\left(1 - \frac{(m+2)\epsilon}{2}\right) \Gamma\left(1 - \frac{(m+1)\epsilon}{2}\right)^2 \Gamma\left(\frac{(m+2)\epsilon}{2}\right)}{16\pi^{2-\epsilon}\Gamma\left(1 - \frac{m\epsilon}{2}\right)} \sum_{n \geq 0} \frac{\Gamma\left(n + \frac{m\epsilon}{2}\right)}{\Gamma\left(n + 2 - \frac{(m+2)\epsilon}{2}\right) \Gamma\left(\frac{(m+2)\epsilon}{2} - n\right)} \frac{(-1)^n}{n!}. \quad (\text{A.10})$$

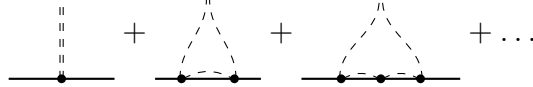
The sum can be written as a hypergeometric function and evaluated to find

$$T_m = \frac{\Gamma\left(1 - \frac{(m+1)\epsilon}{2}\right)^2 \Gamma\left(1 - \frac{(m+2)\epsilon}{2}\right) \Gamma\left(\frac{m\epsilon}{2}\right)}{16\pi^{2-\epsilon}\Gamma(2 - (m+1)\epsilon)}. \quad (\text{A.11})$$

A.2 An all-loop result in $d = 4 - \epsilon$

When the coupling h is small, its beta function is given by (2.10). In this appendix I evaluate the diagrams relevant for determining the beta function at order $h \sim O(\epsilon^0)$ exactly. The leading contribution is the beta function for surface defects of the free $O(N)$ model, and we find that there are no new fixed points of order $h_* \sim O(\epsilon^0)$, in agreement with the bootstrap analysis of [63].

Assuming $h \sim \epsilon^0$, the leading diagrams that contribute to the renormalisation of the defect coupling h are



$$\text{---} \cdot \text{---} + \text{---} \cdot \text{---} + \text{---} \cdot \text{---} + \dots \quad (\text{A.12})$$

Introducing the notation

$$\text{---} \cdot \overset{m}{\text{---}} \cdot \text{---} = (M^\epsilon h_{ij})^m \int d^2\tau_i d^2\tau_{i+1} \frac{C_{d,1}}{|\tau_i - \tau_{i+1}|^{2-m\epsilon}}, \quad (\text{A.13})$$

we have the recursion relation

$$\text{---} \cdot \overset{1}{\text{---}} \cdot \overset{m}{\text{---}} \cdot \text{---} = \frac{C_{d,1}\pi\Gamma\left(\frac{\epsilon}{2}\right)\Gamma\left(\frac{m\epsilon}{2}\right)\Gamma\left(1 - \frac{(m+1)\epsilon}{2}\right)}{\Gamma\left(1 - \frac{\epsilon}{2}\right)\Gamma\left(\frac{(m+1)\epsilon}{2}\right)\Gamma\left(1 - \frac{m\epsilon}{2}\right)} \times \text{---} \cdot \overset{m+1}{\text{---}} \cdot \text{---}. \quad (\text{A.14})$$

The diagram with m legs ending on the defect can then be reduced to the integral

$$(h_{ij})^m \frac{(\pi C_{d,1})^{m-1} \Gamma\left(\frac{\epsilon}{2}\right)^m \Gamma\left(1 - \frac{m\epsilon}{2}\right)}{\Gamma\left(1 - \frac{\epsilon}{2}\right)^m \Gamma\left(\frac{m\epsilon}{2}\right)} \int d^2\tau_1 d^2\tau_m \frac{M^{(m+2)\epsilon} C_{d,1}^3}{|x - \tau_1|^{2-\epsilon} |\tau_1 - \tau_m|^{2-m\epsilon} |x - \tau_m|^{2-\epsilon}}. \quad (\text{A.15})$$

This last integral is T_m (A.7), with the result given in (A.11).

Summing all diagrams (A.12) up to order h^n , we can absorb all the poles in ϵ by taking the counterterm to be

$$\delta h = h \sum_{m=1}^{n-1} \left(\frac{h}{2\pi\epsilon} \right)^m + O(\lambda). \quad (\text{A.16})$$

Taking the limit $n \rightarrow \infty$ and calculating the beta function, we find

$$\beta_{h_{ij}} = -\epsilon h_{ij} + \frac{1}{2\pi} h_{ij} h_{ji} + O(\lambda). \quad (\text{A.17})$$

This is an exact result in h and it agrees with (2.10). Since $\lambda_* \sim O(\epsilon)$ and the beta function must vanish order by order in ϵ at the fixed points, we conclude that also in the interacting theory there are no fixed point of order $O(\epsilon^0)$.

A.3 Renormalisation and defect beta function in 6d

Diagrams	Prefactor	Integral	ϵ -expansion
	$-h$	$\frac{(xM)^\epsilon}{x^2} C_{4-\epsilon,1}$	$\frac{1}{4\pi^2 x^2} + \dots$
	$-\frac{h^2 g_2 + u^2 g_1}{2}$	$\frac{(xM)^{2\epsilon}}{x^2} C_{4-\epsilon,1+\frac{\epsilon}{2}} L_{4-\epsilon}^{(1,1)}$	$\frac{1}{32\pi^4 x^2 \epsilon} + \dots$
	$-\frac{h(Ng_1^2 + g_2^2)}{2}$	$\frac{(xM)^{2\epsilon}}{x^2} C_{4-\epsilon,1+\frac{\epsilon}{2}} L_{6-\epsilon}^{(1,1)}$	$\frac{-1}{768\pi^5 x^2 \epsilon} + \dots$
	$-\frac{h^3 g_2^2 + hu^2 g_1 (g_2 + 2g_1)}{2}$	$\frac{(xM)^{3\epsilon}}{x^2} C_{4-\epsilon,1+\epsilon} L_{4-\epsilon}^{(1,1)} L_{4-\epsilon}^{(1,1+\frac{\epsilon}{2})}$	$\frac{1}{512\pi^6 x^2 \epsilon^2} + \dots$
	$-\delta h$	$\frac{(xM)^\epsilon}{x^2} C_{4-\epsilon,1}$	$\frac{1}{4\pi^2 x^2} + \dots$
	$h\delta_\sigma$	$\frac{(xM)^\epsilon}{x^2} C_{4-\epsilon,1}$	$\frac{1}{4\pi^2 x^2} + \dots$
	$-hg_2\delta h$	$\frac{(xM)^{2\epsilon}}{x^2} C_{4-\epsilon,1+\frac{\epsilon}{2}} L_{4-\epsilon}^{(1,1)}$	$\frac{1}{32\pi^4 x^2 \epsilon} + \dots$

Table 3: Feynman diagrams contributing to the renormalisation of h to order $O(g^2)$. We list the value of the integral of the propagators, its leading pole in the ϵ -expansion, and the overall prefactor of the integral. The values for $C_{d,\alpha}$ and $L_d^{(a,b)}$ are respectively given in (A.3) and (A.2).

In this section I present the calculation of the beta function for the surface defects (4.3). The calculation is performed in the minimal subtraction (MS) scheme, where the counterterms $\delta h, \delta u^i$ absorb poles in ϵ and admit the expansion

$$\delta h = \frac{\delta h^{(1)}}{\epsilon} + \frac{\delta h^{(2)}}{\epsilon^2} + \dots \quad \delta u^i = \frac{(\delta u^i)^{(1)}}{\epsilon} + \frac{(\delta u^i)^{(2)}}{\epsilon^2} + \dots \quad (\text{A.18})$$

Diagrams	Prefactor	Integral	ϵ -expansion
	$-u^i$	$\frac{(xM)^\epsilon}{x^2} C_{4-\epsilon,1}$	$\frac{1}{4\pi^2 x^2} + \dots$
	$-u^i h g_1$	$\frac{(xM)^{2\epsilon}}{x^2} C_{4-\epsilon,1+\frac{\epsilon}{2}} L_{4-\epsilon}^{(1,1)}$	$\frac{1}{32\pi^4 x^2 \epsilon} + \dots$
	$-u^i g_1^2$	$\frac{(xM)^{2\epsilon}}{x^2} C_{4-\epsilon,1+\frac{\epsilon}{2}} L_{6-\epsilon}^{(1,1)}$	$\frac{-1}{768\pi^5 x^2 \epsilon} + \dots$
	$-\frac{u^i (u^2 g_1^2 + h^2 g_1 (g_2 + 2g_1))}{2}$	$\frac{(xM)^{3\epsilon}}{x^2} C_{4-\epsilon,1+\epsilon} L_{4-\epsilon}^{(1,1)} L_{4-\epsilon}^{(1,1+\frac{\epsilon}{2})}$	$\frac{1}{512\pi^6 x^2 \epsilon^2} + \dots$
	$-\delta u^i$	$\frac{(xM)^\epsilon}{x^2} C_{4-\epsilon,1}$	$\frac{1}{4\pi^2 x^2} + \dots$
	$u^i \delta_\varphi$	$\frac{(xM)^\epsilon}{x^2} C_{4-\epsilon,1}$	$\frac{1}{4\pi^2 x^2} + \dots$
	$-(\delta u^i h + u^i \delta h) g_1$	$\frac{(xM)^{2\epsilon}}{x^2} C_{4-\epsilon,1+\frac{\epsilon}{2}} L_{4-\epsilon}^{(1,1)}$	$\frac{1}{32\pi^4 x^2 \epsilon} + \dots$

Table 4: Feynman diagrams contributing to the renormalisation of u^i to order $O(g^2)$. We list the value of the integral of the propagators, its leading pole in the ϵ -expansion, and the overall prefactor of the integral. The values for $C_{d,\alpha}$ and $L_d^{(a,b)}$ are respectively given in (A.3) and (A.2).

The counterterms for the bulk theory have been calculated previously, and here we need [41]

$$\delta_\sigma = -\frac{N g_1^2 + g_2^2}{6(4\pi)^3 \epsilon} + \dots, \quad \delta_\varphi = -\frac{g_1^2}{3(4\pi)^3 \epsilon} + \dots \quad (\text{A.19})$$

Requiring all poles in ϵ to cancel in the 1-point functions for h and u^i fixes the counterterms, and we find

$$\delta h = \frac{1}{\epsilon} \left[-\frac{g_1 u^2 + g_2 h^2}{(4\pi)^2} + \frac{(2g_1 + g_2) g_1 h u^2 + g_2^2 h^3}{2(4\pi)^4} \right] - \frac{1}{\epsilon^2} \frac{(2g_1 + g_2) g_1 h u^2 + g_2^2 h^3}{(4\pi)^4} + O(g^3), \quad (\text{A.20})$$

$$\delta u^i = \frac{u^i}{\epsilon} \left[-\frac{2g_1 h}{(4\pi)^2} + \frac{(2g_1 + g_2) g_1 h^2 + g_1^2 u^2}{2(4\pi)^4} \right] - \frac{u^i (2g_1 + g_2) g_1 h^2 + g_1^2 u^2}{\epsilon^2 (4\pi)^4} + O(g^3). \quad (\text{A.21})$$

From these we can read the beta function. The bare couplings are related to the renormalised couplings via

$$h_0 = M^{\epsilon/2} (h + \delta h) Z_\sigma^{-1/2}, \quad u_0^i = M^{\epsilon/2} (u^i + \delta u^i) Z_\varphi^{-1/2}. \quad (\text{A.22})$$

To obtain the beta function, we take $M \frac{d}{dM} \log h_0$ to get

$$0 = \frac{\epsilon}{2} + \left(\beta_h \frac{\partial}{\partial h} + \beta_{u^i} \frac{\partial}{\partial u^i} + \beta_{g_1} \frac{\partial}{\partial g_1} + \beta_{g_2} \frac{\partial}{\partial g_2} \right) \log \left((h + \delta h) Z_\sigma^{-1/2} \right), \quad (\text{A.23})$$

and similarly for u^i . Working at order $O(g^2)$, we have $\beta_g = -\frac{eg}{2} + \dots$, and we obtain

$$\beta_h = -\frac{\epsilon h}{2} + h\gamma_\sigma + \frac{h}{2}\partial_h\delta h^{(1)} + \frac{g_i}{2}\partial_{g_i}\delta h^{(1)} - \frac{1}{2}\delta h^{(1)} + O(g^3). \quad (\text{A.24})$$

A similar equation holds for β_n . Plugging the value for the counterterms we get (4.4).

References

- [1] A. J. Bray and M. A. Moore, “Critical behaviour of semi-infinite systems,” *Journal of Physics A: Mathematical and General* **10** no. 11, (Nov, 1977) 1927.
- [2] K. Ohno and Y. Okabe, “The $1/N$ expansion for the extraordinary transition of semi-infinite system,” *Progress of Theoretical Physics* **72** no. 4, (10, 1984) 736–745.
- [3] J. L. Cardy, “Conformal invariance and surface critical behavior,” *Nuclear Physics B* **240** no. 4, (1984) 514–532.
- [4] D. M. McAvity and H. Osborn, “Conformal field theories near a boundary in general dimensions,” *Nucl. Phys. B* **455** (1995) 522–576, [arXiv:cond-mat/9505127](#).
- [5] M. E. Fisher and P. G. Gennes, “Wall phenomena in a critical binary mixture,” *Comptes Rendus Hebdomadaires Des Seances De L Academie Des Sciences Serie B* **287** no. 8, (1978) 207–209.
- [6] A. J. Liu and M. E. Fisher, “Universal critical adsorption profile from optical experiments,” *Physical Review A* **40** no. 12, (1989) 7202.
- [7] H. Diehl, “Critical adsorption of fluids and the equivalence of extraordinary to normal surface transitions,” *Berichte der Bunsengesellschaft für physikalische Chemie* **98** no. 3, (1994) 466–471.
- [8] B. M. Law, “Surface amplitude ratios and nucleated wetting near a critical end point,” *Berichte der Bunsengesellschaft für physikalische Chemie* **98** no. 3, (1994) 472–477.
- [9] G. Flöter and S. Dietrich, “Universal amplitudes and profiles for critical adsorption,” *Zeitschrift für Physik B Condensed Matter* **97** (1995) 213–232.
- [10] H. W. Diehl, “The theory of boundary critical phenomena,” *Int. J. Mod. Phys. B* **11** (1997) 3503–3523, [arXiv:cond-mat/9610143](#).
- [11] M. A. Metlitski, “Boundary criticality of the $O(N)$ model in $d = 3$ critically revisited,” *SciPost Phys.* **12** no. 4, (2022) 131, [arXiv:2009.05119](#).
- [12] A. Krishnan and M. A. Metlitski, “A plane defect in the 3d $O(N)$ model,” [arXiv:2301.05728](#).
- [13] E. Eisenriegler and T. W. Burkhardt, “Universal and nonuniversal critical behavior of the n -vector model with a defect plane in the limit $n \rightarrow \infty$,” *Phys. Rev. B* **25** (Mar, 1982) 3283–3291.
- [14] F. Gliozzi, P. Liendo, M. Meineri, and A. Rago, “Boundary and interface CFTs from the conformal bootstrap,” *JHEP* **05** (2015) 036, [arXiv:1502.07217](#).
- [15] P. Dey, T. Hansen, and M. Shpot, “Operator expansions, layer susceptibility and two-point functions in BCFT,” *JHEP* **12** (2020) 051, [arXiv:2006.11253](#).
- [16] T. Nishioka, Y. Okuyama, and S. Shimamori, “Comments on epsilon expansion of the $O(N)$ model with boundary,” *JHEP* **03** (2023) 051, [arXiv:2212.04078](#).
- [17] J. L. Cardy, “Is there a c -theorem in four-dimensions?,” *Phys. Lett. B* **215** (1988) 749–752.

- [18] I. R. Klebanov, S. S. Pufu, and B. R. Safdi, “ F -theorem without supersymmetry,” *JHEP* **10** (2011) 038, [arXiv:1105.4598](#).
- [19] T. Shachar, R. Sinha, and M. Smolkin, “RG flows on two-dimensional spherical defects,” [arXiv:2212.08081](#).
- [20] G. Cuomo, Z. Komargodski, and M. Mezei, “Localized magnetic field in the $O(N)$ model,” *JHEP* **02** (2022) 134, [arXiv:2112.10634](#).
- [21] S. Giombi and H. Khanchandani, “CFT in AdS and boundary RG flows,” *JHEP* **11** (2020) 118, [arXiv:2007.04955](#).
- [22] A. Schwimmer and S. Theisen, “Entanglement entropy, trace anomalies and holography,” *Nucl. Phys. B* **801** (2008) 1–24, [arXiv:0802.1017](#).
- [23] N. Drukker, M. Probst, and M. Trépanier, “Surface operators in the $6d \mathcal{N} = (2, 0)$ theory,” *J. Phys. A* **53** no. 36, (2020) 365401, [arXiv:2003.12372](#).
- [24] C. P. Herzog, K.-W. Huang, and D. V. Vassilevich, “Interface conformal anomalies,” *JHEP* **10** (2020) 132, [arXiv:2005.01689](#).
- [25] K. Jensen and A. O’Bannon, “Constraint on defect and boundary renormalization group flows,” *Phys. Rev. Lett.* **116** no. 9, (2016) 091601, [arXiv:1509.02160](#).
- [26] Y. Wang, “Surface defect, anomalies and b-extremization,” *JHEP* **11** (2021) 122, [arXiv:2012.06574](#).
- [27] L. Bianchi, M. Meineri, R. C. Myers, and M. Smolkin, “Rényi entropy and conformal defects,” *JHEP* **07** (2016) 076, [arXiv:1511.06713](#).
- [28] N. Drukker, M. Probst, and M. Trépanier, “Defect CFT techniques in the $6d \mathcal{N} = (2, 0)$ theory,” *JHEP* **03** (2021) 261, [arXiv:2009.10732](#).
- [29] K. Jensen, A. O’Bannon, B. Robinson, and R. Rodgers, “From the Weyl anomaly to entropy of two-dimensional boundaries and defects,” *Phys. Rev. Lett.* **122** no. 24, (2019) 241602, [arXiv:1812.08745](#).
- [30] A. Lewkowycz and E. Perlmutter, “Universality in the geometric dependence of Rényi entropy,” *JHEP* **01** (2015) 080, [arXiv:1407.8171](#).
- [31] N. Drukker and M. Trépanier, “Ironing out the crease,” *JHEP* **08** (2022) 193, [arXiv:2204.12627](#).
- [32] A. Raviv-Moshe and S. Zhong, “Phases of surface defects in scalar field theories,” [arXiv:2305.11370](#).
- [33] S. Giombi and B. Liu, “Notes on a surface defect in the $O(N)$ model,” [arXiv:2305.11402](#).
- [34] J. Henriksson, “The critical $O(N)$ CFT: Methods and conformal data,” *Phys. Rept.* **1002** (2023) 1–72, [arXiv:2201.09520](#).
- [35] H. Kleinert and V. Schulte-Frohlinde, *Critical properties of ϕ^4 theories*. World Scientific, 2001.
- [36] S. S. Gubser, A. Nellore, S. S. Pufu, and F. D. Rocha, “Thermodynamics and bulk viscosity of approximate black hole duals to finite temperature quantum chromodynamics,” *Phys. Rev. Lett.* **101** (2008) 131601, [arXiv:0804.1950](#).
- [37] V. Gorbenko, S. Rychkov, and B. Zan, “Walking, weak first-order transitions, and complex CFTs,” *JHEP* **10** (2018) 108, [arXiv:1807.11512](#).
- [38] N. Drukker, Z. Kong, and G. Sakkas, “Broken global symmetries and defect conformal manifolds,” *Phys. Rev. Lett.* **129** no. 20, (2022) 201603, [arXiv:2203.17157](#).

- [39] C. P. Herzog and V. Schaub, “The tilting space of boundary conformal field theories,” [arXiv:2301.10789](#).
- [40] M. Moshe and J. Zinn-Justin, “Quantum field theory in the large N limit: a review,” *Phys. Rept.* **385** (2003) 69–228, [arXiv:hep-th/0306133](#).
- [41] L. Fei, S. Giombi, and I. R. Klebanov, “Critical $O(N)$ models in $6 - \epsilon$ dimensions,” *Phys. Rev. D* **90** no. 2, (2014) 025018, [arXiv:1404.1094](#).
- [42] A. Petkou, “Conserved currents, consistency relations and operator product expansions in the conformally invariant $O(N)$ vector model,” *Annals Phys.* **249** (1996) 180–221, [arXiv:hep-th/9410093](#).
- [43] A. C. Petkou, “ $C(T)$ and $C(J)$ up to next-to-leading order in $1/N$ in the conformally invariant $O(N)$ vector model for $2 < d < 4$,” *Phys. Lett. B* **359** (1995) 101–107, [arXiv:hep-th/9506116](#).
- [44] M. Goykhman and M. Smolkin, “Vector model in various dimensions,” *Phys. Rev. D* **102** no. 2, (2020) 025003, [arXiv:1911.08298](#).
- [45] K. Lang and W. Rühl, “The critical $O(N)$ σ -model at dimensions $2 < d < 4$: a list of quasi-primary fields,” *Nuclear Physics B* **402** no. 3, (1993) 573–603. <https://www.sciencedirect.com/science/article/pii/055032139390119A>.
- [46] Y. Deng, H. W. J. Blöte, and M. P. Nightingale, “Surface and bulk transitions in three-dimensional $O(n)$ models,” *Phys. Rev. E* **72** (Jul, 2005) 016128.
- [47] P. Liendo, L. Rastelli, and B. C. van Rees, “The bootstrap program for boundary CFT_d ,” *JHEP* **07** (2013) 113, [arXiv:1210.4258](#).
- [48] L. Fei, S. Giombi, I. R. Klebanov, and G. Tarnopolsky, “Three loop analysis of the critical $O(N)$ models in $6 - \epsilon$ dimensions,” *Phys. Rev. D* **91** no. 4, (2015) 045011, [arXiv:1411.1099](#).
- [49] J. A. Gracey, “Four loop renormalization of ϕ^3 theory in six dimensions,” *Phys. Rev. D* **92** no. 2, (2015) 025012, [arXiv:1506.03357](#).
- [50] M. Kompaniets and A. Pikelner, “Critical exponents from five-loop scalar theory renormalization near six-dimensions,” *Phys. Lett. B* **817** (2021) 136331, [arXiv:2101.10018](#).
- [51] M. Borinsky, J. A. Gracey, M. V. Kompaniets, and O. Schnetz, “Five-loop renormalization of ϕ^3 theory with applications to the Lee-Yang edge singularity and percolation theory,” *Phys. Rev. D* **103** no. 11, (2021) 116024, [arXiv:2103.16224](#).
- [52] D. Rodriguez-Gomez, “A scaling limit for line and surface defects,” *JHEP* **06** (2022) 071, [arXiv:2202.03471](#).
- [53] I. C. n. Bolla, D. Rodriguez-Gomez, and J. G. Russo, “RG flows and stability in defect field theories,” [arXiv:2303.01935](#).
- [54] A. Söderberg Rousu, “Fusion of conformal defects in interacting theories,” [arXiv:2304.10239](#).
- [55] M. Henningson and K. Skenderis, “Weyl anomaly for Wilson surfaces,” *JHEP* **06** (1999) 012, [arXiv:hep-th/9905163](#).
- [56] A. Gustavsson, “Conformal anomaly of Wilson surface observables: a field theoretical computation,” *JHEP* **07** (2004) 074, [arXiv:hep-th/0404150](#).
- [57] S. Gukov and E. Witten, “Gauge theory, ramification, and the geometric Langlands program,” [hep-th/0612073](#).

- [58] A. Pelissetto and E. Vicari, “Critical phenomena and renormalization group theory,” *Phys. Rept.* **368** (2002) 549–727, [arXiv:cond-mat/0012164](#).
- [59] H. Osborn and A. Stergiou, “Seeking fixed points in multiple coupling scalar theories in the ϵ expansion,” *JHEP* **05** (2018) 051, [arXiv:1707.06165](#).
- [60] S. Rychkov and A. Stergiou, “General properties of multiscalar RG flows in $d = 4 - \epsilon$,” *SciPost Phys.* **6** no. 1, (2019) 008, [arXiv:1810.10541](#).
- [61] W. H. Pannell and A. Stergiou, “Line defect RG flows in the ϵ expansion,” [arXiv:2302.14069](#).
- [62] I. R. Klebanov and A. M. Polyakov, “AdS dual of the critical $O(N)$ vector model,” *Phys. Lett. B* **550** (2002) 213–219, [arXiv:hep-th/0210114](#).
- [63] E. Lauria, P. Liendo, B. C. Van Rees, and X. Zhao, “Line and surface defects for the free scalar field,” *JHEP* **01** (2021) 060, [arXiv:2005.02413](#).